Photoluminescence from site-selected coupling between quantum dots and microtoroid cavities

Xiaowei Wu (吴晓伟)[1], Changling Zou (邹长铃)[1], Wei Wei (尉 伟)[2], Fangwen Sun (孙方稳)[1*], Guangcan Guo (郭光灿)[1], and Zhengfu Han (韩正甫)[1]**

[1]*Key Laboratory of Quantum Information, University of Science and Technology of China, Hefei 230026, China*
[2]*National Synchrotron Radiation Laboratory, University of Science and Technology of China, Hefei 230029, China*
[*]*E-mail: fwsun@ustc.edu.cn;* [**]*e-mail: zfhan@ustc.edu.cn*

Received December 23, 2009

By using CdSe/ZnS quantum dots (QDs), we study the effect of cavity quantum electrodynamics on the coupling of the microtoroid cavity. When with whispering gallery (WG) modes, the microtoroid cavity demonstrates high quality factor and small mode volume at visible wavelengths. Accordingly, fiber tapers allow QDs to adhere into the cavity and further permit the control of site-selected coupling. From the luminescence spectra, QDs are modulated effectively by cavity modes. Variable modulations are observed by changing QD coupling conditions. Therefore, based on experimental and theoretical research, strong and tunable Purcell enhancement can be realized by this system.

OCIS codes: 020.5580, 140.3945, 060.2310.
doi: 10.3788/COL20100807.0709.

In recent years, due to their small mode volume and high quality factor (Q), various types of microcavities have been studied for low threshold laser[1], high sensitive sensing[2], and optomechanics[3]. Microcavities have performed well in test platforms and experiments for cavity quantum electrodynamics (QED)[4,5]. However, studies on cavity QED have shown limitations in terms of adjusting coupling conditions between the atom and cavity. Atom-like systems, such as quantum dots (QDs)[6,7], diamond crystals[8], and dye molecules[9], are usually located at fixed positions in microcavities. This condition has further limited their use in sample preparations, particularly, when adjusting single photon emitters.

Fiber tapers[10] could efficiently couple the light passing in and out of a microcavity in an evanescent field. They could also excite and collect the luminescence of atom-like emitters using near-field coupling[11], which could further provide for controlled coupling of QDs and light in cavity QED experiments. In this letter, we demonstrate the site-selected coupling of few QDs and microtoroid cavities using a fiber taper. From the system, direct tuning of QD emission is observed.

Colloidal QDs, such as CdSe/ZnS, have advantages of easy synthesis, convenient manipulation, and strong binding-energy-induced luminescence at room temperature. Thus, they are appropriate in the study of cavity QEDs. In preparing the sample, and by keeping the emission at 610 nm, CdSe/ZnS colloidal QDs were dispersed in toluene to a density of approximately 20 μm^{-3}. To allow for adherence and detection of QDs, we fabricated a fiber taper by heating and pulling a standard fiber to a diameter of less than 1 μm at the taper. Breaking the fiber taper, such that its tip had a diameter of around 10 μm (Fig. 1(a)), ensured the precise positioning of the QDs at the fiber taper. QDs were first adhered to the fiber tip by dip coating. Then, the tip with QDs was scratched vertically onto the fiber taper at a certain position. The narrow width of the tip and low quantity of QDs ensured the adherence of QDs onto the fiber taper. QDs concentrated only on a tiny spot, the number of which was estimated at less than 10. Upon attachment, QD photoluminescence was observed by band-pass filter when the fiber was pumped with 532-nm laser. Figures 1(b) and (c) demonstrate the fluorescent images of QDs in dark field and weak bright field, respectively. The location was marked on the monitor following coupling to the microtoroid cavity. For this operation, it is feasible to attach even a single QD[12] at a certain location to realize strong coupling[13,14] at a microcavity mode.

Experiment was performed using the setup shown in Fig. 2(a). In the experiment, the silica microtoroid cavity[15] with whispering gallery (WG) mode was utilized to couple the QDs. Before preparing the microtoroid, the microdisk[16,17] was fabricated using the standard photolithograph process combined with gas etching technology. Next, the microdisk

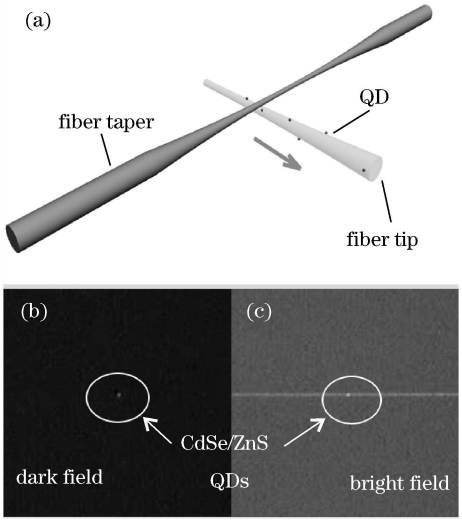

Fig. 1. (a) Demonstration for the process of adhering several QDs into a fiber taper; (b), (c) images of the same QDs on fiber taper at dark field and bright field, respectively.

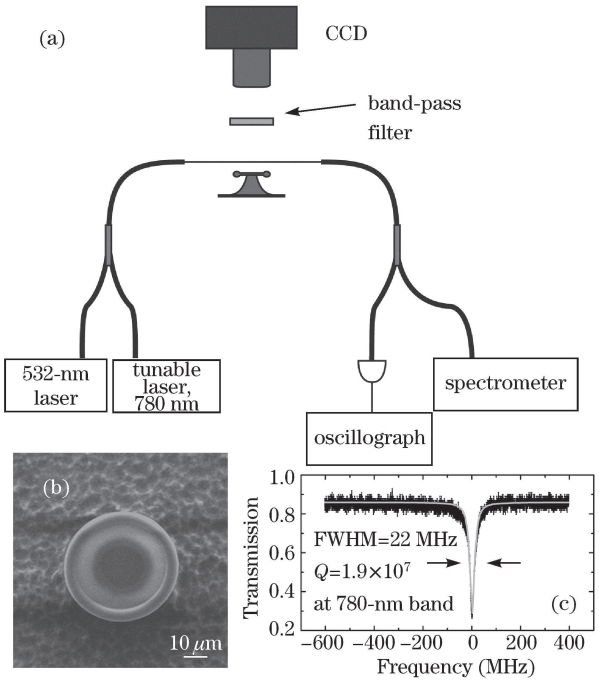

Fig. 2. (a) Experimental setup of coupling system. The tunable laser is used to survey the quality factor of the microtoroid, and the 532-nm laser is utilized as a pump source to excite QDs. (b) SEM image of a microtoroid cavity. (c) Experimentally measured transmission spectrum with the microtoroid. The dip corresponds to the WG mode, and the quality factor of the mode reached 1.9×10^7. CCD: charge-coupled device.

was reflowed by laser pulse heating to generate a toroidal cavity. Fig. 2(b) shows a scanning electron microscopy (SEM) image of the top view of a microtoroid. The heat-melted edge of the microdisk and surface-tension-induced smooth toroidal shapes, which then reduced the surface roughness and scattering of a microcavity. To realize coupling between QDs and microtoroid, the latter was employed for three-dimensional (3D) piezoelectric transition (PZT) at a position accuracy of 20 nm. In doing so, the gap between the fiber taper and the microtoroid allowed for precise adjustments. As demonstrated in the experiment setup (Fig. 2(a)), we used a tunable laser (780-nm band) to survey the quality factor by combining a photon detector to receive the transmitted signal and an oscillograph to obtain the transmission spectrum. Similarly, to detect the luminescence of QDs, we used the 532-nm laser as pump light and a spectrometer to measure the spectrum.

As previously mentioned, the heat-melting fabricated microtoroid cavity was with a smooth surface, which diminished scattering loss from etching-induced surface defects. Hence, the quality factor was raised instead of the microdisk cavity[17]. Meanwhile, the mode volume had not increased much due to proper geometry definition (i.e., very small edge side provides good light confinement in the vertical direction), which indicated the advantageous contribution of the microtoroid in the study of cavity QED. Figure 2(c) shows the measured transmission spectrum of a microtoroid of the the dip presenting absorption from the WG mode. The full-width at half-maximum (FWHM) was estimated at 22 MHz based on the fitting with Lorentz line shape; the value corresponded to 1.9×10^7 for the cavity mode at 780-nm band wavelength.

We then fixed the fiber taper according to the marked QDs in the monitor (the arrow indicates the position in the right inset of Fig. 3). Subsequently, a microtoroid was operated to approach the position of QDs. We excited the QDs using a 532-nm laser through the evanescent field from the fiber taper where the emitted luminescence was also collected. QDs on the surface of the fiber taper without cavity tuning sometimes retains photon emission in free space. The surveyed luminescence is exhibited as a spectrum (i) in Fig. 3. The luminescence of QDs exhibited a Gaussian shape around the region of 610 nm. The experiment was performed at room temperature. QDs achieved significant inhomogeneous broadening effect, which has led to the broad linewidth of the spectrum (FWHM $\sim$ 20 nm).

QDs can be moved into the field range of WG modes by adjusting the air gap between the microtoroid and fiber tape. Photon emission rate can be enhanced by the Purcell effect[18] when the frequency is resonant with the cavity mode, while photon emission is eliminated for the transition when the frequency is mismatched. The enhanced intensity is higher than the luminescence from QDs on a bare taper. In the experiment, we changed the relative position of QDs and microtoroid. The original Gaussian shape peak was influenced by the modulated spectrum over the detected range with a series of sharp peaks in the Lorentz type (Fig. 3, spectrum (ii)). The peaks followed the same wavelength interval corresponding to the free spectral range (FSR) of the WG modes. Beyond the main peaks, when we tuned the position of microtoroid, many short peaks from other high order WG modes also appeared, the intensity of which depended on

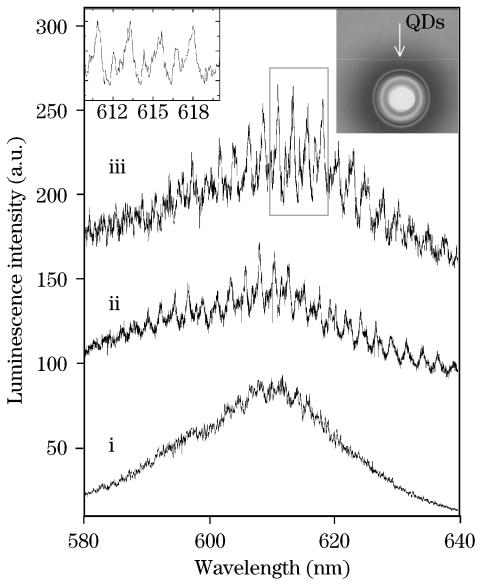

Fig. 3. Spectra of QDs collected from the fiber taper. By using site-selected coupling with the microtoroid, the distance between the toroid and fiber taper is adjusted from (i) farther away to (ii) a nearer position, until final (iii) contact. Meanwhile, the modulated patterns for QDs are changed. Unsymmetrical peak pattern is shown in the left inset; the top view of the system during the coupling process is shown in the right inset.

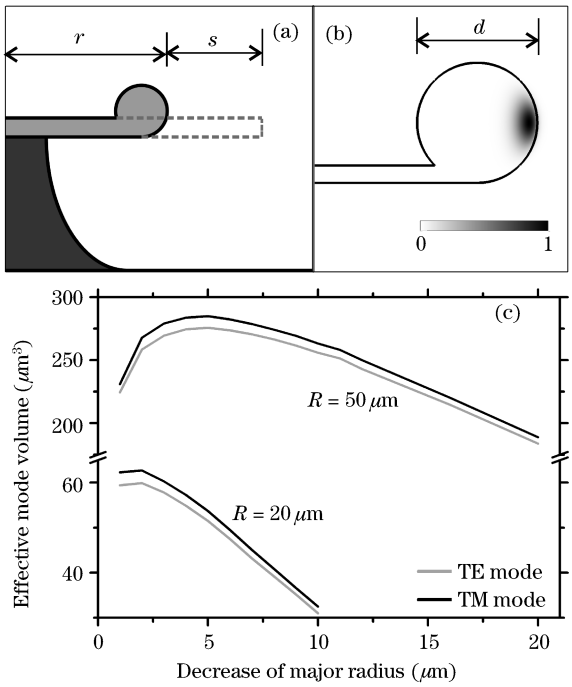

Fig. 4. Definition of a microtoroid shape in cross section. It demonstrates that the radius shrinks from a disk to a toroid outline. (b) Field distribution of a ground TE mode in the microtoroid at a normalized intensity. (c) Variation of effective mode volume versus the major radius decrease. Different cases of R=50 and 20 μm are demonstrated with their TE and TM modes, respectively.

the efficiency of coupling among cavity mode, QDs, and fiber taper.

By coordinating the position of the microtoroid, the cavity achieved different modulations for emitted luminescence. Generally, the variation of the WG mode field provides different Purcell enhancements for QDs, and the change of the coupling efficiency relates to photons collection[19]. The modulated peaks achieved different intensities, as can be seen by comparing the spectra of (ii) and (iii) in Fig. 3, due to different cavity positions. However, the FSR of the ground mode was almost constant. In this coupled system, with microtoroid coupling, photons emitted from QDs obtained two feasible traveling paths. On one hand, the photons were directly coupled into the fiber taper and were transmitted; on the other hand, photons were coupled into the microcavity under a proper near-resonance coupling condition, and then returned to the fiber taper. We determined these two transmission paths using the mode distribution of the microcavity, as well as by the mutual coupling conditions among QD, cavity, and fiber taper. From these two paths, we observed the spectra in the fiber involving the superposition of luminescence. Owing to the microtoroid, the FSR of the cavity was constant; this allowed us to determine the photons through which the two paths were modulated (i.e., the same FSR, but with different phases and modulation amplitudes). The interference through the two paths marked the Fano line shape in the spectrum[20]. As shown in spectrum (iii) of Fig. 3, some peaks obtained unsymmetrical shapes (left inset) that do not follow a Lorentz peak. QDs in our experiment were not a single emitter, and the coherent property could be interrupted by multiple QD emissions that weaken Fano-like resonances. In the spectrum, an overlap with the high order WG mode could influence the unsymmetrical peak. In the experiment, photon collection was strongly associated with the diameter of the fiber taper. Thinner fiber tapers provide better collecting efficiency of QDs. However, transmission loss should still be considered.

In theory, the mode of microtoroid cavity can be studied as a toroid-shaped cavity combined with a round planar substrate. In our analysis of the cross section of a microtoroid (Fig. 4(a)), the original microdisk was shrunk in diameter to generate a toroidal edge. We defined the former major radius of the microdisk as $R = r + s$, where r is the outer radius of toroid and s is the decrease of major radius. For the toroidal edge, due to surface tension, the cross section was approximately circle-shaped with a minor diameter of d. Following the actual parameters of the microtoroid, which was reflowed from an R=50 μm microdisk (1 μm in thickness) to almost r=30 μm in radius. We calculated the spatial mode distribution of ground TE mode at 610 nm (Fig. 4(b)) with the field intensity being normalized. The mode volume was 188.7 μm^3.

The high quality factor microtoroid cavity could theoretically provide remarkable Purcell enhancement (about 580) at the maximum field. Usually, the Purcell factor is related to the quality factor Q of a microcavity and effective mode volume $V_{\rm eff}$ of a cavity mode. This could be described as

$$F = \frac{3}{4\pi^2}\frac{Q}{V_{\rm eff}}\left(\frac{\lambda}{n_{\rm eff}}\right)^3 \psi, \tag{1}$$

where

$$\psi = \sum_i \frac{|E_i|^2}{|E_0|^2} \tag{2}$$

is the electric field at which QD is located and E_0 is the maximum[5]. Equation (1) shows that the wavelength and quality factor can be fixed depending on chosen cavity and QD. Consequently, the Purcell factor could strongly correlate with the location of QD in the electric field, which is linked with variations in ψ. QDs inside the microtoroid could reach better enhancement because the field is highly confined in the cavity (Fig. 4(b)). Accordingly, we coupled the QDs through multilayer coating[21].

Owing to the special shape of the microtoroid, the change of $V_{\rm eff}$ was affected by the decrease in the major radius. We used standard microdisks with the major radii of 50 and 20 μm to investigate $V_{\rm eff}$ of the microtoroid. Results are shown in Fig. 4(c). For both microtoroids, with the decrease in major radius, $V_{\rm eff}$ first increases, after which it drops with the radius. $V_{\rm eff}$ is defined by both r and d; therefore, when the radius decreases in the reflow process, r reduces its size, and d expands gradually. However, in the further reduction of major radius, r takes on the main effect.

In conclusion, site-selected coupling between a few CdSe/ZnS QDs and high quality factor WG modes in microtoroid has been realized. We have observed the Purcell effect modulated emission spectra from QDs, and

the unique WG modes in a microtoroid cavity are also characterized theoretically. Site-selected coupling using the fiber taper has been demonstrated as convenient and efficient. Moreover, this method is believed to be valuable for other microcavity structures. For future cavity QED experiments, the technique can achieve controllable operations when a single QD is coupled into cavity modes, subsequently improving coupling and detecting efficiency.

The authors thank Jinming Cui and Chunhua Dong for their helpful discussion. This work was supported by the National Fundamental Research Program of China (No. 2006CB921900), the National Natural Science Foundation of China (Nos. 60537020 and 60621064), and the Knowledge Innovation Project of the Chinese Academy of Sciences.

References

1. L. Yang, D. K. Armani, and K. J. Vahala, Appl. Phys. Lett. **83,** 825 (2003).
2. A. M. Armani and K. J. Vahala, Opt. Lett. **31,** 1896 (2006).
3. T. Carmon, H. Rokhsari, L. Yang, T. J. Kippenberg, and K. J. Vahala, Phys. Rev. Lett. **94,** 223902 (2005).
4. P. Michler, A. Kiraz, C. Becher, W. V. Schoenfeld, P. M. Petroff, L. Zhang, E. Hu, and A. Imamoğlu, Science **290,** 2282 (2000).
5. M. Makarova, V. Sih, J. Warga, R. Li, L. D. Negro, and J. Vuckovic, Appl. Phys. Lett. **92,** 161107 (2008).
6. C. Becher, A. Kiraz, P. Michler, A. Imamoğlu, W. V. Schoenfeld, P. M. Petroff, L. Zhang, and E. Hu, Phys. Rev. B **63,** 121312(R) (2001).
7. Y.-Z. Huang, K.-J. Che, Y.-D. Yang, S.-J. Wang, Y. Du, and Z.-C. Fan, Opt. Lett. **33,** 2170 (2008).
8. A. Beveratos, R. Brouri, T. Gacoin, J. P. Poizat, and P. Grangier, Phys. Rev. A **64,** 061802(R) (2001).
9. H. Yanagi, R. Takeaki, S. Tomita, A. Ishizumi, F. Sasaki, K. Yamashita, and K. Oe, Appl. Phys. Lett. **95,** 033306 (2009).
10. L. Tong, R. R. Gattass, J. B. Ashcom, S. He, J. Lou, M. Shen, I. Maxwell, and E. Mazur, Nature **426,** 816 (2003).
11. K. P. Nayak and K. Hakuta, New J. Phys. **10,** 053003 (2008).
12. P. Michler, A. Imamoğlu, M. D. Mason, P. J. Carson, G. F. Strouse, and S. K. Buratto, Nature **406,** 968 (2000).
13. J. McKeever, A. Boca, A. D. Boozer, J. R. Buck, and H. J. Kimble, Nature **425,** 268 (2003).
14. T. Yoshie, A. Scherer, J. Hendrickson, G. Khitrova, H. M. Gibbs, G. Rupper, C. Ell, O. B. Shchekin, and D. G. Deppe, Nature **432,** 200 (2004).
15. D. K. Armani, T. J. Kippenberg, S. M. Spillane, and K. J. Vahala, Nature **421,** 925 (2003).
16. T. J. Kippenberg, S. M. Spillane, D. K. Armani, and K. J. Vahala, Appl. Phys. Lett. **83,** 797 (2003).
17. X. Wu, Y. Xiao, Y. Yang, C. Dong, Z. Han, and G. Guo, Chin. Opt. Lett. **5,** 668 (2007).
18. J. M. Gérard, B. Sermage, B. Gayral, B. Legrand, E. Costard, and V. Thierry-Mieg, Phys. Rev. Lett. **81,** 1110 (1998).
19. M. Cai, O. Painter, and K. J. Vahala, Phys. Rev. Lett. **85,** 74 (2000).
20. P. E. Barclay, C. Santori, K.-M. Fu, R. G. Beausoleil, and O. Painter, Opt. Express **17,** 8081 (2009).
21. C.-H. Dong, F.-W. Sun, C.-L. Zou, X.-F. Ren, G.-C. Guo, and Z.-F. Han, Appl. Phys. Lett. **96,** 061106 (2010).